

# 1 Human lncRNAs harbor conserved modules embedded 2 in different sequence contexts

3 Francesco Ballesio<sup>1</sup>, Gerardo Pepe<sup>2</sup>, Gabriele Ausiello<sup>2</sup>, Andrea Novelletto<sup>2</sup>, Manuela Helmer-  
4 Citterich<sup>2,\*</sup>, Pier Federico Gherardini<sup>2,\*</sup>

5

6 <sup>1</sup> PhD Program in Cellular and Molecular Biology, Department of Biology, University of Rome "Tor  
7 Vergata", Rome, Italy.

8 <sup>2</sup> Department of Biology, University of Rome "Tor Vergata", Rome, Italy.

9

10 \* To whom correspondence should be addressed. Tel: 00390672594324; Fax:0039062023500; Email:  
11 citterich@uniroma2.it; Email: pier.federico.gherardini@uniroma2.it

12

13

14

15

## 16 Abstract

17

18 We analyzed the structure of human long non-coding RNA (lncRNAs) genes to investigate  
19 whether the non-coding transcriptome is organized in modular domains, as is the case for protein-coding  
20 genes. To this aim, we compared all known human lncRNA exons and identified 340 pairs of exons with  
21 high sequence and/or secondary structure similarity but embedded in a dissimilar sequence context.  
22 We grouped these pairs in 106 clusters based on their reciprocal similarities. These shared modules are  
23 highly conserved between humans and the four great ape species, display evidence of purifying  
24 selection and likely arose as a result of recent segmental duplications. Our analysis contributes to the  
25 understanding of the mechanisms driving the evolution of the non-coding genome and suggests  
26 additional strategies towards deciphering the functional complexity of this class of molecules.

27

## 28 **Author summary**

29

30           The Human genome includes more than 18,000 genes coding for RNAs that are not translated  
31 into proteins, called long non-coding RNAs (lncRNA). Mounting evolutionary and experimental evidence  
32 shows that a large amount of these RNAs have a specific function, mainly as regulators of a diverse set  
33 of biological processes. Here we set out to investigate whether these genes have a modular organization  
34 similar to that of protein-coding genes. Accordingly, we compared the sequence of all the exonic regions  
35 of human lncRNAs and identified 106 clusters of non-repetitive exonic modules shared between this  
36 class of genes. These modules display evidence of purifying selection, are highly conserved between  
37 humans and the four great ape species, and may represent distinct functional units that have been  
38 shuffled among multiple lncRNA genes, in a manner similar to the exon-shuffling process that is  
39 observed in the coding genome.

## 40 Introduction

41

42 Many eukaryotic proteins are composed of a discrete number of domains, endowed with  
43 autonomous folding capacity and/or characteristic functions. This type of organization is defined as  
44 modular, and the process by which this set of modules is recombined into a variety of different protein  
45 products is known as "exon-shuffling" [1].

46 Long noncoding RNAs (lncRNAs) represent a heterogeneous class of RNAs that are not  
47 translated into functional protein products but, similar to messenger RNAs, are transcribed from genes  
48 that may have an exon/intron structure. These RNAs are generally defined as non-coding RNAs of more  
49 than 200 nucleotides in length and can be capped, polyadenylated and spliced [2], much in the same  
50 way as the transcripts of protein coding genes. The human genome contains about 18,000 lncRNA  
51 genes and 47,000 transcripts [3], most of which are of unknown function. lncRNAs exhibit evidence of  
52 purifying selection and experimental evidence shows that at least a portion of them is indeed functional  
53 (287 eukaryotic lncRNAs associated with a biological function are collected by [4], 1,273 human  
54 lncRNAs by [5]). Some lncRNAs have been characterized in depth and they may function as regulatory  
55 molecules both in the nucleus and the cytoplasm, through a variety of mechanisms, including interaction  
56 with transcription factors, recruitment of chromatin modifying complexes, modulation of the expression  
57 of their neighboring genes, control of mRNA stability and translation and competition for the binding of  
58 specific miRNAs [6–8]. Individual lncRNAs have been found to have a role in promotion of metastasis  
59 [9], neuronal differentiation [10], regulation of the accumulation of beta amyloid peptide in Alzheimer's  
60 disease [11], and many other processes in a diverse array of pathological and physiological contexts.  
61 However the identification of the function of lncRNAs on a global scale remains elusive [12], also  
62 because their definition likely encompasses an extremely heterogeneous set of genes, whose main, and  
63 possibly only, common characteristic is the fact that they do not produce a functional protein product  
64 [13].

65 In general, lncRNAs are significantly less conserved than protein-coding sequences [14], which  
66 also suggests that the relationship between sequence and function is particularly complex in this class  
67 of molecules. Examples of lncRNA such as *Xist*, *Megamind*, *Cyrano* and *Miat* have been described,  
68 which have conserved functions throughout multiple organisms, and yet display a level of sequence  
69 divergence that challenges sequence homology search tools [13,15]. A corollary of this observation is

70 that similarity amongst lncRNA within a given organism is also limited, and, unlike coding sequences,  
71 most lncRNAs appear in single copies in vertebrate genomes [13].

72 However, lncRNAs are significantly more likely to contain repetitive sequences, particularly  
73 transposable elements (TEs) [15,16]. On one hand, this could simply indicate that lncRNAs are more  
74 prone to transposon insertion, because of their aforementioned looser association between sequence  
75 and function [13]. On the other hand, this observation implies the existence of stretches of homologous  
76 sequences that are shared among different lncRNAs, even when the lncRNAs themselves are not  
77 related by descent.

78 Because TEs are often enriched in sequences with regulatory function, and may contribute to  
79 their “spread” within a genome [17], Johnson and Guigò [18] hypothesized that the presence of TEs  
80 may result in the sharing of functional cassettes among evolutionarily unrelated lncRNA, possibly  
81 implying a modularization of function for this class of molecules [6,12], reminiscent of the notion of  
82 domains in the protein-coding world. In support of this hypothesis, it has been reported that TE-derived  
83 sequences within lncRNAs are more conserved compared with non-TE sequences [19].

84 Here we set out to expand the identification of modules in lncRNAs that could have contributed  
85 to increasing the diversity of the non-coding genome, similar to the exon-shuffling phenomenon that is  
86 well known for protein sequences. Our work extends previous observations in three ways, namely by i)  
87 focusing on the sharing of individual exons among unrelated lncRNAs within the human genome, ii)  
88 specifically excluding exons that contain repetitive sequences, and iii) including secondary structure as  
89 an additional criterion to define similarity, as lncRNAs with similar functions often lack linear sequence  
90 homology [20], and many examples of ncRNA are known whose function is tied to their secondary  
91 structure [21–24].

92

## 93 **Results**

94

### 95 **Exon sequence and secondary structure comparison**

96

97 In order to search for similarities among lncRNAs, we performed a pairwise comparison of both  
98 the sequence and the predicted secondary structure of 12,097 non-overlapping human lncRNA exons

99 that do not contain repetitive sequences, performing a total of more than 73 million sequence alignments  
100 and an equal number of structure alignments. The distributions of the corresponding scores are shown  
101 in Figure 1A, B (1A-B Fig.).

102 To identify pairs or groups of exons representing shared sequence elements, hereafter referred  
103 to as "modules", it was necessary to select a threshold above which their sequence or structure similarity  
104 would be considered significant.

105 We thus investigated the conservation of lncRNA exons in four non-human primates (see  
106 Materials and Methods), with the goal of identifying shared sequence elements in the human genome  
107 that are also conserved in other primate genomes.

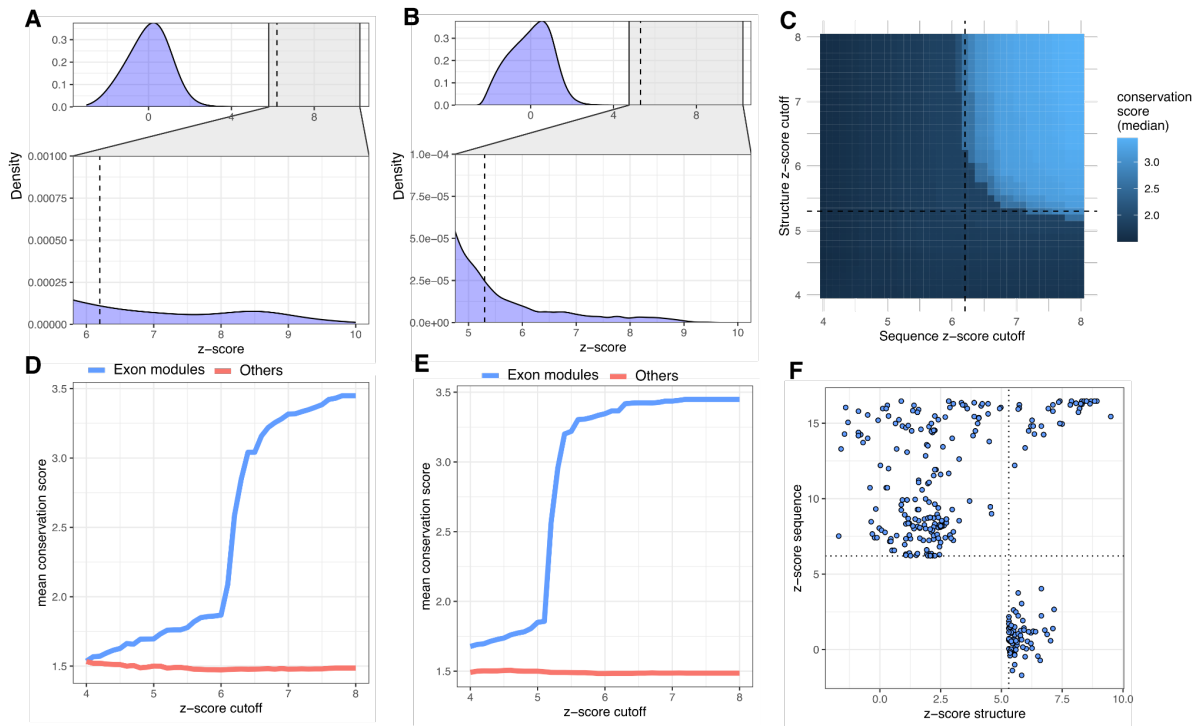
108 Accordingly, we calculated the mean conservation scores of sequence modules across these  
109 species, as a function of the similarity score threshold used to define the modules themselves. Using  
110 this procedure, we observed a sharp transition in conservation at Z-score similarity thresholds of 6.2  
111 and 5.3 for sequence and structure alignments, respectively (1C-D-E Fig.). We consider this increase in  
112 conservation, coupled with the high Z-score similarity threshold, as a strong indication that the shared  
113 sequence elements we identified represent significant similarities. As a further benchmark, we repeated  
114 the entire procedure by aligning exons against random sequences with the same length and base  
115 composition. None of the alignments produced z-scores above the 6.2 threshold.

116 By using these thresholds, we identified a total of 340 exon pairs (219 identified by sequence,  
117 75 by structure and 46 by both), involving 338 different exons and 218 different genes (1F Fig.). Starting  
118 from these pairwise similarities, we identified 106 clusters (exon modules) defined by homologous  
119 lncRNA exons represented in at least two copies in the same or different genes (2 Fig., S1 Fig. and S1  
120 Table).

121 To rule out the possibility that similarity between exons in a pair of genes is simply due to  
122 paralogy, we aligned the entire genes using BLAST and excluded pairs with alignment coverage on the  
123 smallest gene of the pair greater than 80%. Measuring the alignment coverage of the entire genes,  
124 including introns, allowed us to identify and exclude cases of complete paralogy even in the presence  
125 of intronization or imprecise exon annotation.

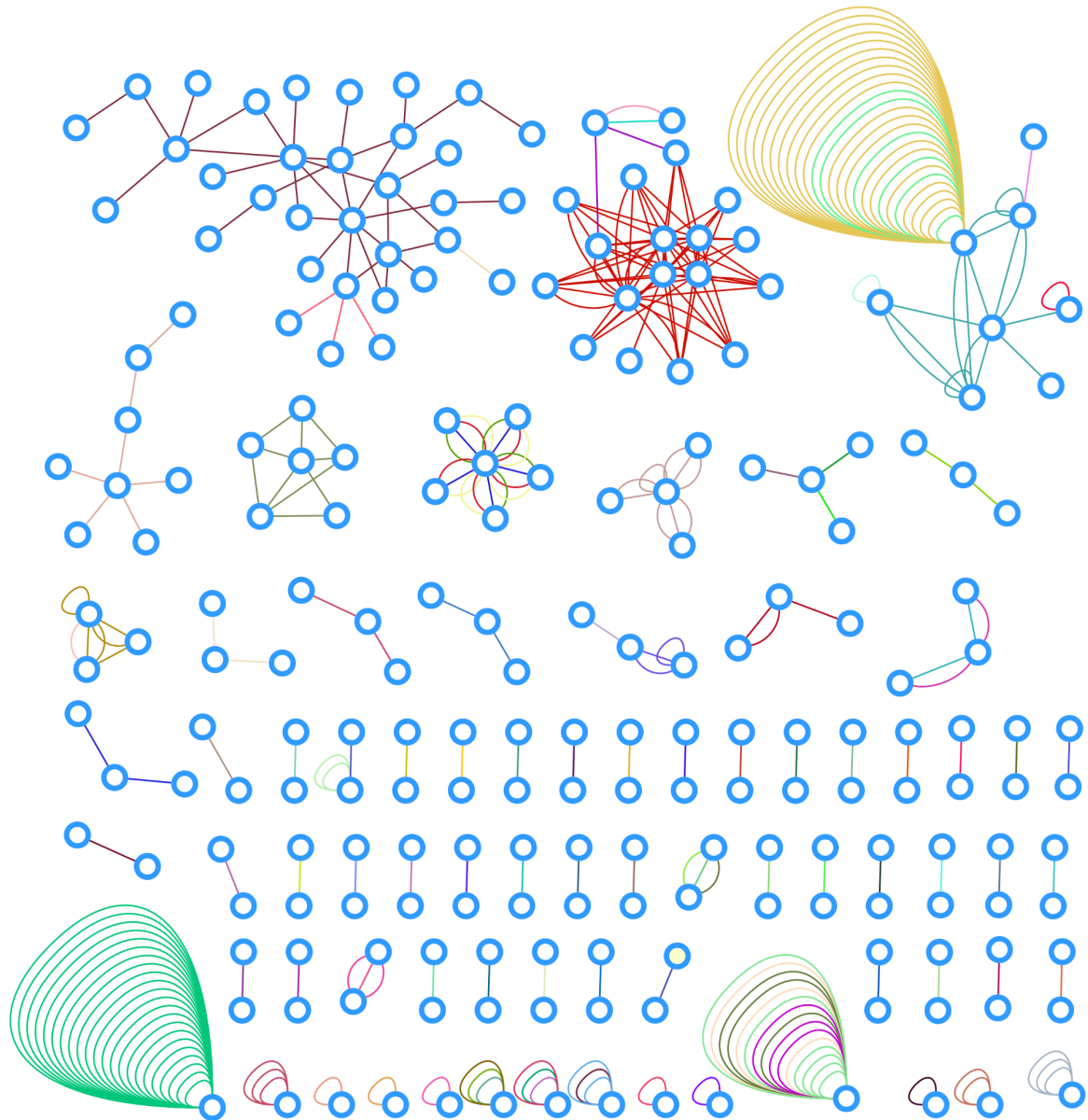
126 We note that, in general, our analysis is dependent on the reliability of the reconstruction of the  
127 whole transcript structure, which is used to define the exons themselves. This is summarized by the  
128 Transcript Support Level (TSL, S1 Table).

129



130

131 **Fig.1 Sequence and structure alignments results.** A) Distribution of z-transformed pairwise  
132 alignment scores for sequence; B) Distribution of z-transformed pairwise alignment scores for structures,  
133 for these distributions, a close-up around the proposed cutoff thresholds is also shown; C) heatmap  
134 representing the conservation scores in the four non-human primates of all pairs selected at the different  
135 z-score thresholds of sequence and structure alignments; D, E) Mean conservation scores (within four  
136 non-human primates) of members of clusters defined by different z-score thresholds of pairwise  
137 similarity for sequence (D) and structure (E). Note the steep increase in evolutionary conservation for  
138 the z-score cutoff of 6.2 (sequence) and 5.3 (structure), respectively; F) Scatter plot of sequence and  
139 structure similarity z-scores of the exon pairs (for the sake of clarity, the more than 73 million pairs below  
140 the thresholds are not shown).



141

142 **Fig.2 Network representation of the exon-sharing gene clusters and the corresponding**

143 **exon modules.** Each node represents a lncRNA gene and each edge an exonic module shared

144 between two genes. Same color edges within a gene cluster represent a module. Self-loops represent

145 instances where the same module occurs multiple times in a single gene. The network representation

146 was generated using Cytoscape [25].

147

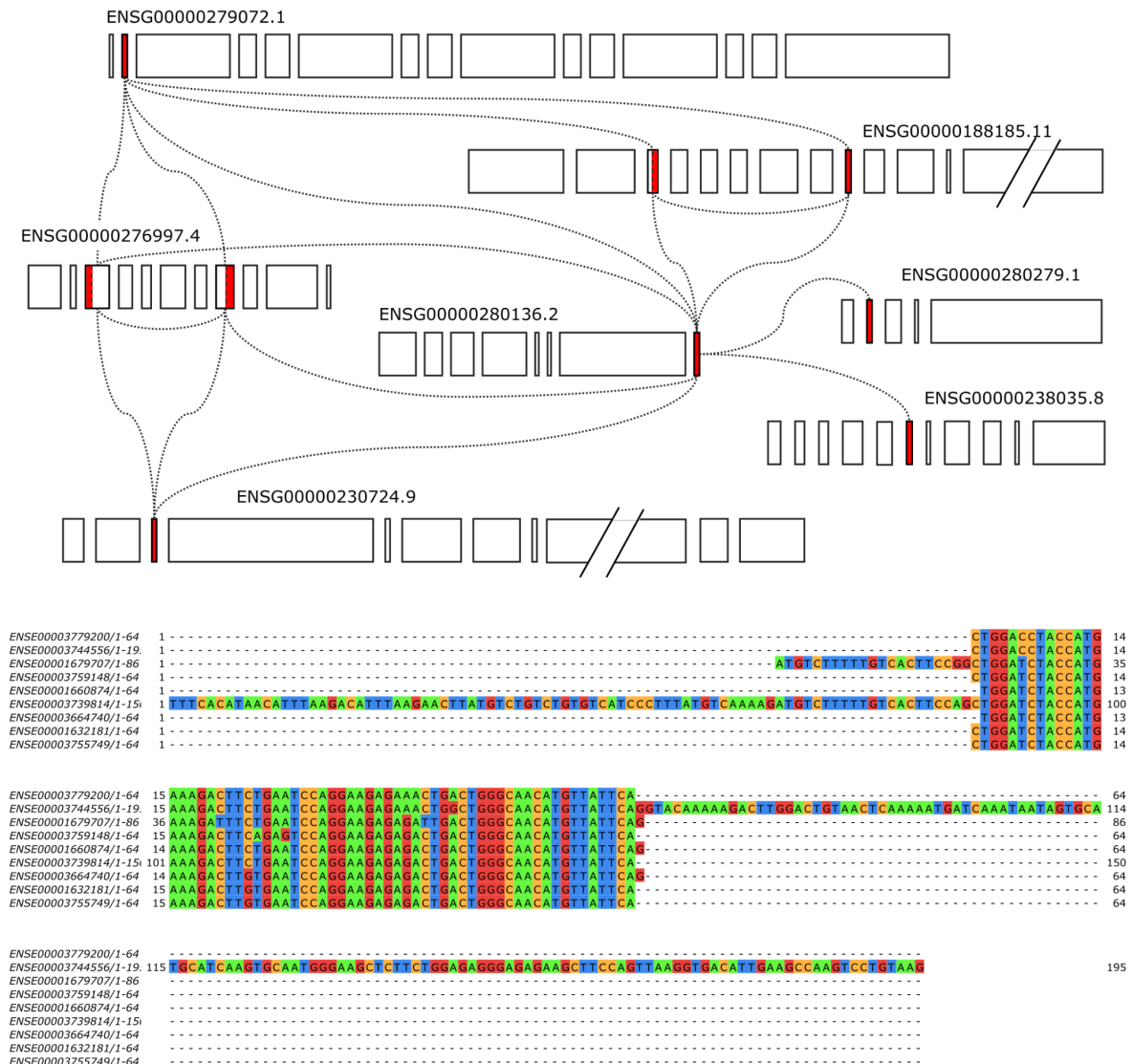
148 Figure 3A (3A Fig.) is an example of one of the identified exon modules shared by a group of 7

149 lncRNA genes: ENSG00000279072.1, ENSG00000188185.11, ENSG00000276997.4,

150 ENSG00000280136.2, ENSG00000280279.1, ENSG00000230724.9, ENSG00000238035.8. This

151 cluster consists of 9 exons that contain a region of ~65 nucleotides with high sequence similarity

152 (external gap trimmed sequence identity 92-98%, 3B Fig.) embedded in different genes. It is worth noting  
 153 that, in some cases, the module constitutes an exon on its own, whereas in other cases it is part of a  
 154 larger exon.  
 155



156  
 157 **Fig.3 An example of the identified exon modules.** A) Schematic representation of 7 genes  
 158 containing representatives (in red) of exons contributing to a module cluster. Each box represents an  
 159 exon, with width proportional to its length (intron length not to scale); B) multiple alignment of the 9 exons  
 160 contributing to the cluster.

161  
 162 We then analyzed in more detail the sequence context of exon modules. More specifically, we  
 163 looked at the sequence similarity of additional exons flanking the modules, to rule out the possibility that

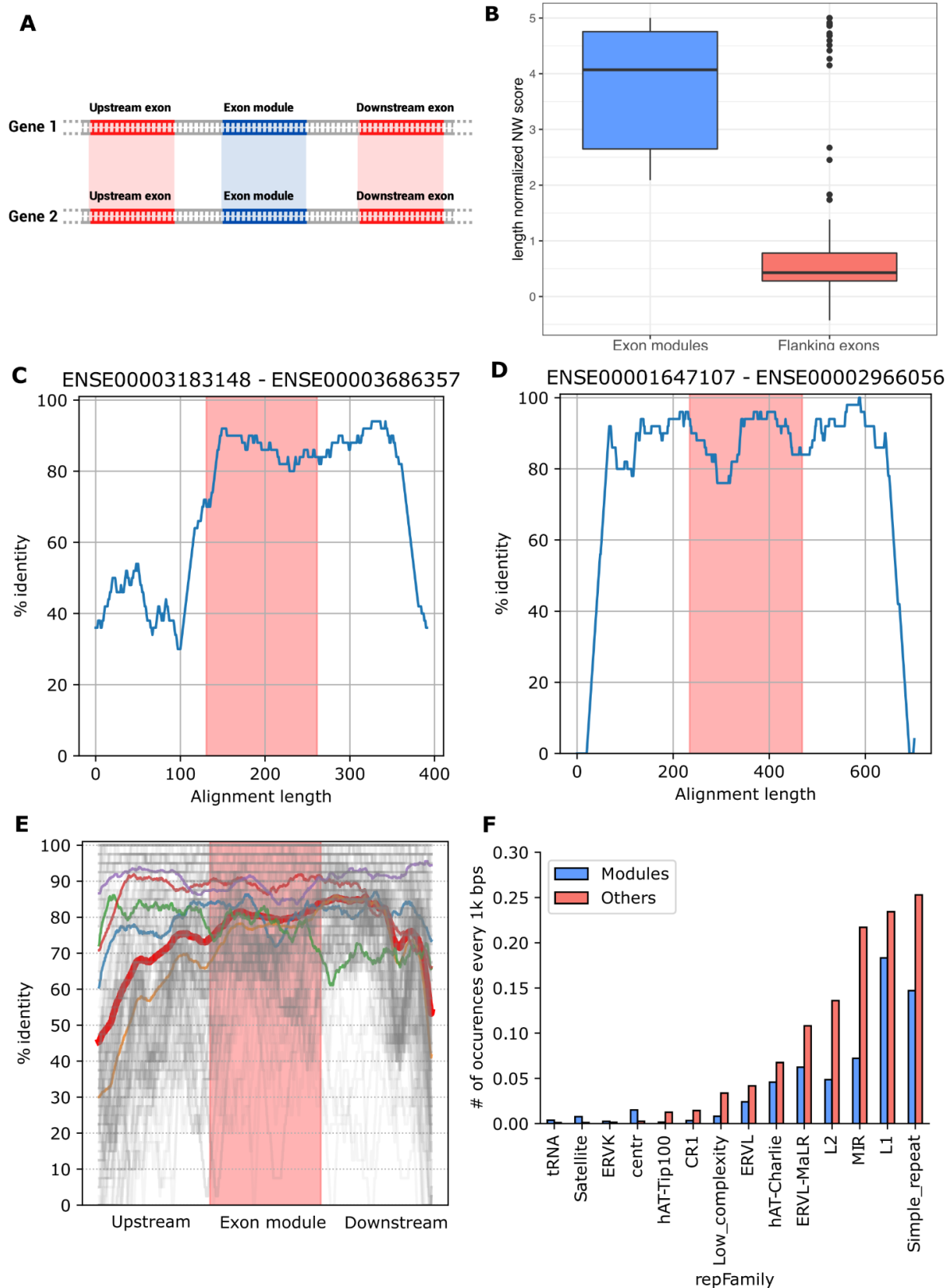


164 the similarity between modules in different genes simply reflects global sequence similarity between the  
165 exonic components of genes (see Materials and Methods and 4A Fig.). The alignment scores for exons  
166 flanking the putative module in the same gene, upstream and downstream (4B Fig.), showed that the  
167 similarity between exon modules is significantly higher than that of the sequence context in which they  
168 are embedded. We also observed a small proportion of cases in which the flanking exons are also similar  
169 (outliers in 4B Fig.). These cases fall outside the criteria used to define exon modules: in 17 cases  
170 because they are less than 50 nucleotides in length, and in another 17 cases because they contain  
171 repetitive sequences.

172 We then analyzed the sequence similarity of the intronic sequences flanking the exon modules.  
173 To this end, we defined genomic regions of interest by extending upstream and downstream the  
174 sequence of each candidate exon pair, until we obtained two sequences with a length equal to three  
175 times that of the longest exon of the pair (4C-E Fig.). We limited the analysis to pairs with sequence  
176 similarity above the z-score threshold of 6.2 and excluded modules repeating within the same gene. For  
177 each pair of genomic regions of interest, we performed a global alignment using the same parameters  
178 used to identify the exon modules, and calculated the percentage identity of the pairs using overlapping  
179 windows of 50 nucleotides with a single nucleotide shift, to generate graphs depicting the extent of the  
180 similarity. We found that, in the majority of instances, sequence similarity extends into the flanking  
181 intronic regions. More specifically, in approximately one third of the cases, the similarity encompassed  
182 both the upstream and downstream intron, in another third of the cases the similarity extended to a  
183 single intron, while the remainder of cases lacked a clear pattern. We did not observe any cases where  
184 the similarity was confined to the boundaries of the candidate exon modules.

185 The extension of the similarity through the flanking introns suggests that the most common  
186 mechanism responsible for the origin of exon modules is segmental duplication of a genomic DNA  
187 stretch encompassing the parental copy of an exon. This is the same mechanism suggested as a driver  
188 of exon shuffling in protein coding genes [26]. To further confirm these findings, we compared our results  
189 with the data present in the UCSC Segmental Dups track (genomicSuperDups) which contains regions  
190 detected as putative genomic duplications within the human genome. These regions represent large  
191 recent duplications ( $\geq 1$  kb and  $\geq 90\%$  identity) that originated over the last ~40 million years of  
192 human evolution, based on neutral expectation of divergence [26]. For 84 of the 340 lncRNA exon pairs

193 identified here, we found a match in the segmental duplications identified by Bailey et al. In 81 of these  
194 cases the duplicated stretch includes the entire exons of the pair, while in 3 cases the duplication is  
195 interrupted within the exon. We also observed a higher frequency of pairs located on the same  
196 chromosome (~20.5%) compared with what is observed when the same exons are randomly paired  
197 (~3.6%). Moreover, pairs of exon modules that are on the same chromosome are closer together when  
198 compared to the same random pairing control (Mann-Whitney p-value=9.86e-05). A higher rate of  
199 occurrence on the same chromosome has been described for segmental duplications [27]. To further  
200 extend the analysis of flanking regions, we compared the rate of occurrence of multiple families of  
201 repetitive elements in the introns flanking candidate exonic modules vs other lncRNA exons (for exons  
202 located at the ends of a gene, we included a region of 10k bps in the genome). We calculated the  
203 number of occurrences per 1,000 base pairs of each family of repetitive elements on the set of regions  
204 flanking the exon modules vs the other lncRNA exons (4F Fig., S2 Table) thus obtaining a distribution  
205 of occurrences where the observations correspond to the individual sequence regions. We then  
206 compared these distributions using a Mann-Whitney U test, with Bonferroni correction for multiple  
207 hypothesis testing. We observed significant differences for 15 of 46 families (padj<0.05). Interestingly,  
208 centromere and satellite repeats are among the few classes of repeats enriched in regions flanking the  
209 exon modules, while most classes of transposon- or endogenous retrovirus-derived repeats are  
210 depleted. Since the genomic regions proximal to centromeres and telomeres are enriched with  
211 segmental duplications [28], this observation further points at segmental duplication as the main driver  
212 of the appearance of these exon modules, as opposed to, for instance, transposition. The enrichment  
213 of this type of repetitive sequences can be explained by the localization near the centromeres or  
214 telomeres of a portion of the modules (S2 Fig.). Moreover, searching for transposase domains using a  
215 procedure similar to the one described in [29] did not reveal significant differences in their occurrence  
216 among genes containing exon modules (data not shown), further highlighting that transposition is not  
217 the main driver of this process.



218

219

220

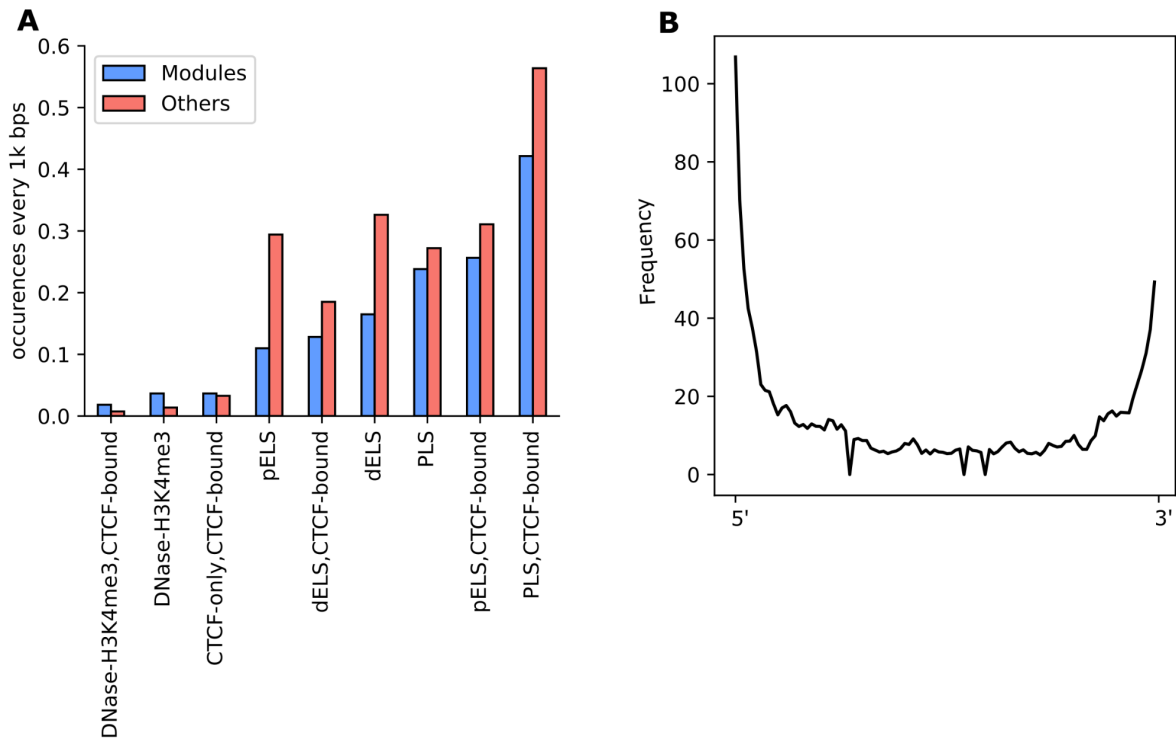
**Fig.4 Analysis of the sequence regions flanking exon modules.** A) For each pair of genes containing a shared exon module we compared the similarities of the upstream and downstream flanking

221 exons (when present); B) Distributions of the length-normalized Needleman and Wunsch scores of  
222 exonic modules (in blue) and of their upstream and downstream flanking exons (in red); C) A pair of  
223 exons in which the similarity only extends to the downstream flanking intron; D) A pair of exons in which  
224 the similarity extends upstream and downstream into both flanking introns; E) Overall representation of  
225 all the length-scaled similarities between all the exon pairs and their flanking introns (in grey), the median  
226 identity percentage is represented in red. The other colored lines represent five clusters of similarity  
227 patterns as defined by grouping individual lines; F) Number of occurrences per thousand base pairs of  
228 families of repetitive sequences in flanking introns with significant differences ( $p_{adj} < 0.05$ ) between the  
229 exonic modules and the other lncRNA exons.

230

231

232 To further investigate the characteristics of these modules we looked at the distribution of cis-  
233 regulatory elements (CRE) within their sequences (5A Fig.). This research highlighted a depletion in  
234 exon modules of the most frequent CREs (Fisher's exact test  $p_{adj} = 6.2e10^{-3}$ ,  $1.2e10^{-2}$ ,  $1.2e10^{-2}$  for  
235 pELS, dELS and PLS, CTCF-bound respectively). One of the few elements that are not depleted are  
236 H3K4me3 marks, which are characteristic of transcriptionally active regions (Howe et al. 2017).  
237 Interestingly this histone modification is usually found in the region corresponding to the beginning of  
238 the transcript [30]. Accordingly, when we investigated the position of the exonic modules within their  
239 transcripts (5B Fig.), we detected a higher frequency of the modules at the 5' end. This finding is  
240 consistent with what is observed in protein coding genes, which in vertebrates tend to increase their  
241 length over time by gaining recently evolved domains, primarily through the addition of sequences at  
242 the 5' end of genes [31]. The insertion of these modules at the extremities of the transcript presumably  
243 allows the addition of genetic material with minimal disruption to the existing sequence.



244

245 **Fig 5 Cis-regulatory elements (CRE) and position of the modules.** A) number of  
246 occurrences of the different CREs from the annotation present in ENCODE every thousand nucleotides  
247 in the modules (in blue) and in the other lncRNA exons of the dataset (in red); B) the y axis indicates  
248 the frequency of regions containing modules relative to their position on their transcript (which is  
249 indicated on the Y axis, see Methods), as the sum of modules present in that region. The higher y value  
250 therefore indicates that there is a greater number of modules at the ends of the transcripts, particularly  
251 at the level of the 5' end.

252

## 253 Evolutionary conservation of exon modules

254

255 To analyze in detail the inter-specific conservation of exon modules, we compared their  
256 conservation scores (see Materials and Methods) with the conservation scores of functionally annotated  
257 lncRNA exons, using the conservation scores of other lncRNA exons as control. Functionally annotated  
258 lncRNA genes were collected from the lnc2Cancer database [5], which contains experimentally  
259 supported annotations of lncRNA associated with a biological function, as derived from the literature  
260 (see Materials and Methods). The comparison of these three categories revealed that the conservation  
261 score of exon modules was higher than that of exons belonging to functionally annotated lncRNA genes

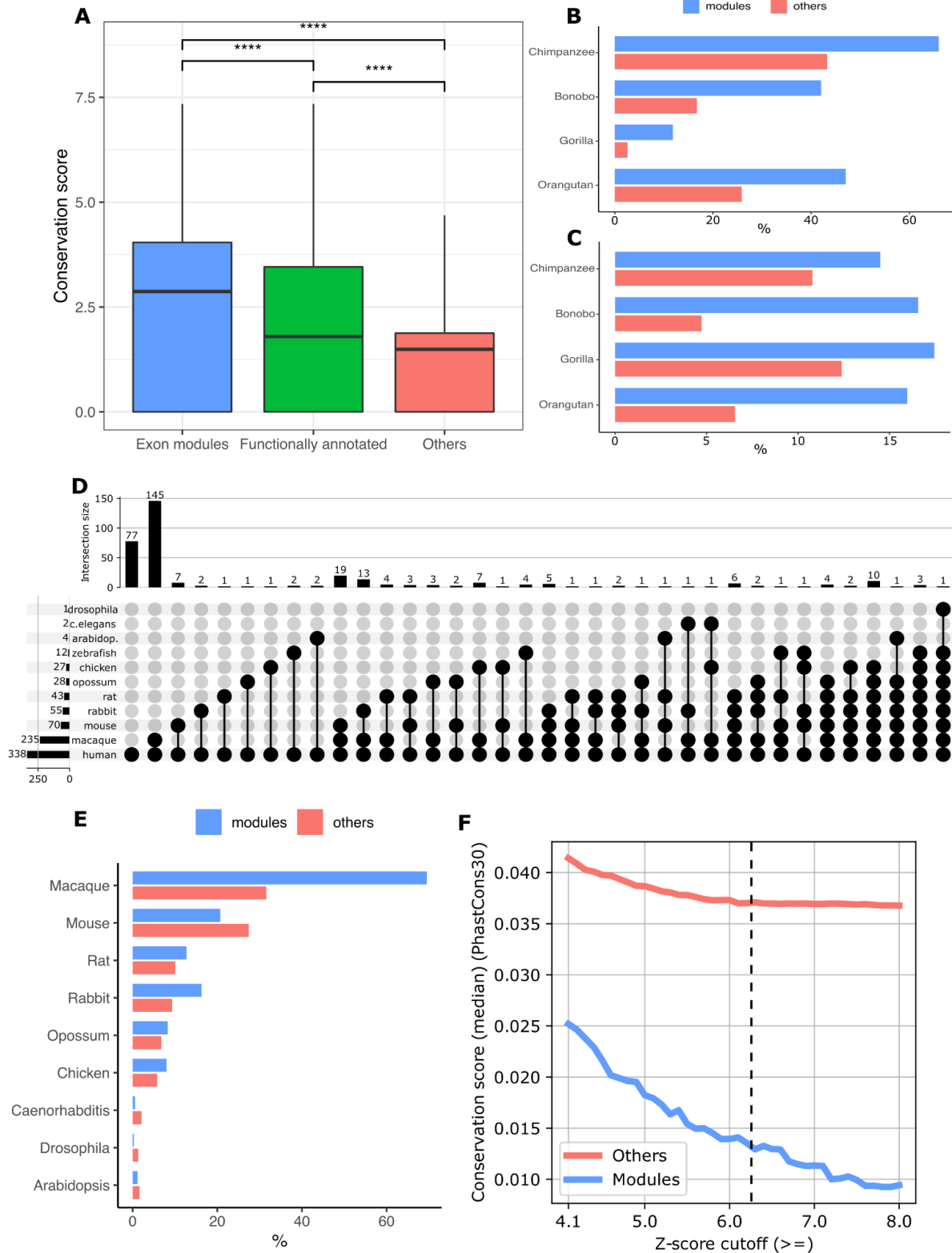
262 (Mann-Whitney  $p$ -value=6.3e-5), and both the conservation score of exon modules and of exons  
263 belonging to functionally annotated lncRNA were significantly higher than the conservation score of the  
264 remaining lncRNA exons (Mann-Whitney  $p$ -value=7.4e-27 and 3.5e-26 respectively, 6A Fig.). When  
265 looking at the conservation of exon modules in four higher primate species, we also observed a greater  
266 proportion of exons with a BLAST hit among exon modules vs the remaining exons. More specifically,  
267 65.97% of the exon modules have a BLAST hit in Chimpanzee, 42.01% in Bonobo, 11.83% in Gorilla  
268 and 47.04% in Orangutan. Conversely, only 43.23%, 16.72%, 2.61%, 25.86% of the control exons (i.e.  
269 the portion of the 12097 lncRNA exons that have no repetitive and non-overlapping sequences and that  
270 are not modules) have BLAST hits on the same species respectively (6B Fig.) To evaluate the  
271 significance of these results we performed a Fisher's exact test on the aggregated data from the different  
272 species, which confirmed that these results are significant ( $p$ -value=4.10e-15).

273         Since the BLAST similarity score with non-human primates does not take into account the  
274 genomic position of exons in different organisms, i.e. it cannot distinguish between the similarity of true  
275 orthologs vs in- and out- paralogs, we investigated whether exon modules are located in regions of  
276 synteny between non-human primates more often than other exons. To this end we leveraged the  
277 SynthDB [32] database, which provides data on orthology relationships between humans and other  
278 primates. We observed that the percentage of genes located in a syntenic region is higher for genes  
279 that contain at least one exon module, compared with those which do not. Accordingly, 14.50% of the  
280 exon modules are located in genes that have an ortholog in Chimpanzee, 16.57% in Bonobo, 17.46%  
281 in Gorilla and 15.98% in Orangutan. While for the other lncRNA exons we observed percentages of  
282 10.79, 4.74, 12.39, 6.55 in the same species respectively. We then performed a Fisher's exact test  
283 comparing exons modules that belong to genes with an ortholog in at least one of the species mentioned  
284 above to the other exons which confirmed the significance of our results ( $p$ -value=5.63e-05) (6C Fig.).

285         To strengthen the evolutionary conservation analysis, and to compare our results with the  
286 analysis by Sarropoulos et al. 2019 [33], we extended it by including additional species. To this end, we  
287 aligned all lncRNA exons using blastn against the genomes of the organisms used in Sarropoulos et al.  
288 2019 (Macaque, taxid: 9544; Rabbit, taxid: 9986; Chicken, taxid: 9031; Opossum, taxid: 13616; Rat,  
289 taxid: 10116; Mouse, taxid: 10090), and other model organisms (Danio rerio, taxid: 7955; Drosophila  
290 melanogaster, taxid: 7227; Caenorhabditis elegans, taxid: 6239; Arabidopsis thaliana, taxid: 3702),  
291 using an e-value threshold of 0.01 to identify hits (5D-E Fig., S3 Fig.). Figure 6E (6E Fig.) displays the

292 percentage of exonic modules vs other lncRNA exons that have at least one hit in the species indicated  
293 above. This analysis shows a rapid decay in the number of similar exons as the evolutionary distance  
294 from humans increases. Figure 5F (5F Fig.) shows the 30 mammal PhastCons scores of the exon  
295 modules, as a function of the z-score similarity threshold used to define the modules themselves (i.e.  
296 the threshold described in 1A Fig.). This analysis demonstrates that the exon modules identified in this  
297 work, which are highly similar as they were selected on the basis of having a Z-score of at least 6.2 and  
298 5.3 in the sequence and structure alignment respectively, represent duplications that are recent (as  
299 implied by the high levels of sequence similarity) and that are exclusively found in humans and higher  
300 primates, and thus have lower PhastCons scores on the entire set of 30 mammals (6F Fig.) .

301 Overall, the above results reveal that roughly 4% of lncRNA genes (218 lncRNA genes/5,423  
302 total lncRNAs genes which contain at least one exon without repetitive sequences, see Materials and  
303 Methods) include one or more exons having significant similarity with exonic portions of other lncRNAs.  
304 To our knowledge, this represents the first draft of a genome-wide catalog of shared lncRNA exons.



305

306

**Fig.6 Evolutionary conservation of exon modules.** A) Box-plot of the conservation scores in

307 four non-human primates for exon modules, functionally annotated exons from the Inc2Cancer

308 database, and controls; B) Percentage of exon modules (in blue) and other exons (in red) that showed

309 a BLAST hit (e-value <0.001) in the primate species considered; C) Percentage of genes showing a



310 conserved syntenic region (as defined in SynthDB) among those containing exon modules (in blue) vs  
311 genes not containing an exon module (in red); D) Upset plot representing the exons that have a BLAST  
312 hit in the species analyzed in Sarropoulos et al. and in other model organisms; E) Percentages of  
313 modules (in blue) and other exons (in red) showing a BLAST hit in the indicated species F) PhastCons  
314 30 mammals scores of members of clusters defined by different z-score thresholds of pairwise similarity  
315 from sequence alignments (in blue) and the other lncRNA exons of the dataset (in red).

316

## 317 Nucleotide variation in modules

318

319 To further investigate whether exon modules may represent conserved functional units, we  
320 analyzed the occurrence and frequency of single nucleotide polymorphisms (SNPs) in these regions, as  
321 a lower incidence of variants may indicate the existence of constraints associated with functional  
322 sequences, due to the effects of purifying selection [34]. Accordingly, we collected SNP data from the  
323 1000 Genome project from dbSNP 153 [35] and we observed 12.87 variants per thousand bases in  
324 control exons (which are not modules) and 11.83 in modules. We then obtained from the ALFA allele  
325 frequencies aggregator [36] a total of 764,005 SNPs located in lncRNA exons, [36] and their associated  
326 frequencies. For each exon, we calculated the index of nucleotide diversity  $\theta\pi$  [37] as

$$327 \theta\pi = \frac{\sum_{i=1}^l 2f_i(1-f_i)}{l}$$

328 where  $f_i$  represents the frequency of variants in the  $i$ th position of the exon sequence in the population,  
329 and  $l$  represents the length of the exon.

330 After comparing the distributions of  $\theta\pi$  scores with the Mann-Whitney U test, we obtained a p-  
331 value of 2.14e-02 in the comparison between modules and exons from functionally annotated genes, a  
332 p-value of 2.77e-02 from the comparison between exon modules and other lncRNA exons and a non-  
333 significant p-value (7.45e-01) from the comparison between functionally annotated and others,  
334 confirming a significant lower propensity to harbor variation in exon modules as compared to the other  
335 two groups. These findings indicate the existence of evolutionary constraints which limit the occurrence  
336 of variants with polymorphic frequencies in exon modules, which in turn may reduce the rate of  
337 evolutionary change in the long-term. We also looked at the frequency of polymorphic complete exon  
338 deletions, but the results were not statistically significant (data not shown).

339

## 340 **Search for characteristics shared with protein coding genes**

341

342 To confirm that exon modules do not simply represent mis-annotated protein domains, we  
343 compared their sequence characteristics with those of known coding genes.

344 França et al. [38] observed that symmetric shuffling units (exons whose length is an exact  
345 multiple of three) are strongly over-represented in human protein coding genes, due to their lower impact  
346 on the reading frame when transposed. We found an opposite trend in lncRNA exon modules, with only  
347 25% having a length that is a multiple of three, which confirms the lack of relevance of the reading frame.  
348 By contrast, in the remainder of the exons, this proportion is 33%, i.e. what would be expected under a  
349 random model.

350 The transition/transversion ratio ( $T_i/t_v$ ) among polymorphic variants should be 0.5 under a purely  
351 random model, resulting from four possible transitions/eight possible transversions. However, real data  
352 depart remarkably from this expectation, with functional regions and protein coding regions presenting  
353 values higher than 0.5, since transitions are more likely to result in non-synonymous substitutions (e.g.  
354 when they occur in the third base of a codon) [39]. Exon modules displayed values of 1.9, in line with  
355 previous results for lncRNAs [40]. As a reference, these values contrast sharply with those for protein  
356 coding genes, which range between 2.8-2.9 +/- 0.1 [40].

357

358

## 359 **Functional hypothesis and organization of putative modules**

### 360 **in clusters of lncRNA genes**

361

362 To further describe exon modules, here we show some examples of their organization within  
363 the structure of their lncRNA genes. Only 12 of 218 genes containing exon modules are associated with  
364 a known biological function in the lnc2Cancer database [5]. For most of them, the specific region of the  
365 lncRNA molecule responsible for that function is unknown. In the next two paragraphs we will provide a  
366 more detailed description for two of the identified modules, in an attempt to capture their putative

367 functions. The first example refers to an exon module recognized by virtue of sequence similarity, and  
368 the second one refers to an exon module recognized by virtue of structure similarity.

369

## 370 **Identification of a putative YBX1 binding module**

371

372 Figure 7A (7A Fig.) shows an example of a putative module represented in a pair of exons as a  
373 sequence of ~200 nucleotides sharing a high sequence similarity (>87%). The exons involved are  
374 ENSE00003710224.1 and ENSE00003838358.1 which belong to genes ENSG00000182165.17 (also  
375 known as TP53TG1) and ENSG00000285540.1, respectively. TP53TG1 is a lncRNA involved in the p53  
376 network response to DNA damage [41], which has a role as tumor suppressor by blocking the  
377 tumorigenic activity of the RNA binding protein (RBP) YBX1 [42]. More in detail, the expression of  
378 TP53TG1 is induced by p53 under cellular stress conditions that involve the induction of double-strand  
379 breaks [41], while the interaction in the cytoplasm between TP53TG1 and YBX1 prevents the migration  
380 of the latter inside the nucleus where it might promote the transcription of a series of oncogenes [43].  
381 *Diaz-Lagares et al.* [42] demonstrated that a central region of TP53TG1, which includes the putative  
382 module in the exon ENSE00003710224.1, is responsible for YBX1 binding. Moreover, they proved that  
383 YBX1 binding motifs CACC are necessary to ensure the tumor-suppressor function of TP53TG1. We  
384 identified two occurrences of the CACC motif in ENSE00003710224.1 and one in ENSE00003838358.1,  
385 suggesting a common role for this module.

386

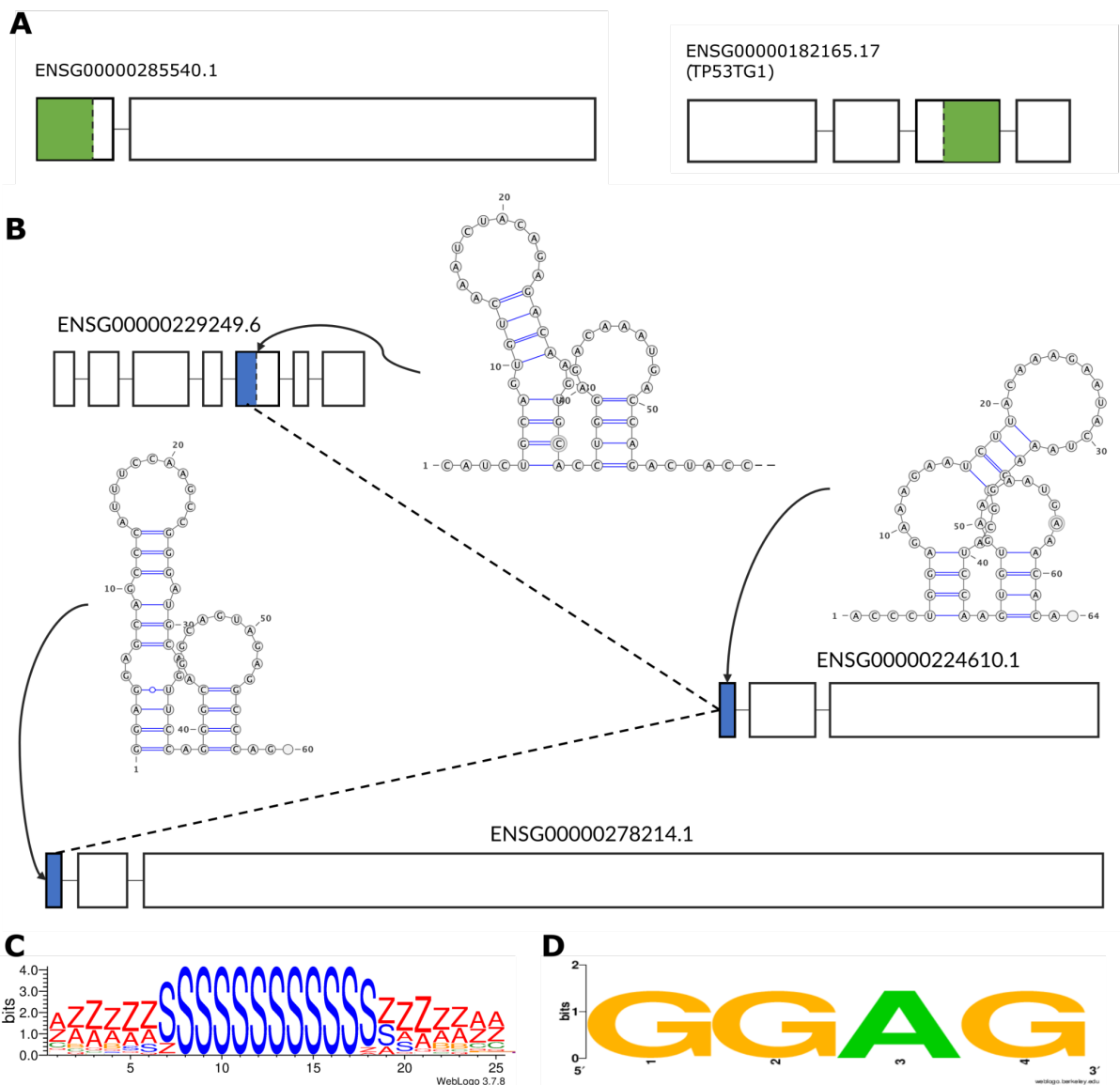
## 387 **Identification of a putative LIN28B binding module**

388

389 Figure 7B-D (7B-D Fig.) shows an example of a module with high structure similarity, embedded  
390 in dissimilar sequence contexts. The exons involved are ENSE00003741285.1, ENSE00001800736.1  
391 and ENSE00001782399.1 which belong to ENSG00000278214.1, ENSG00000224610.1 and  
392 ENSG00000229249.6, respectively (7B Fig.). These three exons fold into a similar secondary structure,  
393 composed of two stems ending with a hairpin loop, with one of the two stems having one or two internal  
394 loops.

395 To detect a possible function, common to the three representatives of this exon module, we  
396 searched for the presence of enriched structure and sequence motifs using the BRIO web server (see

397 Materials and Methods). BRIO identified a significantly enriched (Fisher's exact test  $p < 0.05$ ) structure  
 398 motif shared between all the exons of the group (7C Fig.). This particular motif was associated by Adinolfi  
 399 *et al.* [44] with a series of different RNAs capable of binding some RBPs including LIN28B. This is an  
 400 evolutionary conserved RBP involved in several cellular processes, which acts as a critical oncogene  
 401 activated in cancer [45]. LIN28B is known to be able to bind different mRNAs, including a set of mRNAs  
 402 for splicing factors [46], miRNAs [47] and lncRNAs such as NEAT1 [48]. Furthermore, LIN28B C-terminal  
 403 zinc knuckle (ZnK) mediates specific binding to a conserved GGAG motif [49] which is also a sequence  
 404 motif present in all the three representatives of this module (7D Fig.). These observations suggest a  
 405 possible role of this module in binding LIN28B.



406

407

408           **Fig.7 Organization of a sequence and a structure module and identified motifs.** A)  
409 Schematic representation of the lncRNA genes containing the putative YBX1 binding module (in green);  
410 B) Representation of the lncRNA genes containing the exons with the putative LIN28B binding module  
411 and their secondary structures. The blue boxes represent the exons with high structural similarity that  
412 form the module; C) secondary structure motif revealed by BRIO represented with the BEAR alphabet  
413 [50]; D) sequence motif recognized by ZnK in the three modules. The RNA secondary structure  
414 representations were generated using VARNA (Darty et al. 2009); Sequence and structure logos were  
415 generated using WebLogo [51].  
416

## 417 **Discussion**

418  
419           This work identified a set of lncRNA exons with high sequence and/or structure similarity that  
420 are embedded within globally dissimilar genes, confirming the hypothesis of exon sharing between this  
421 class of molecules similar to protein-coding genes. This set contains a total of 340 pairs of exons that  
422 can be grouped, on the basis of their reciprocal connections, in 106 clusters. In contrast to previous  
423 work [18], our analysis focused on exons that do not contain repetitive sequences. The resulting dataset  
424 of exon modules likely represents the result of recent segmental duplications that are almost exclusively  
425 found in humans and higher primates. These findings support the hypothesis that the non-coding  
426 transcriptome is structured into modular domains, similar to the organization observed in protein-coding  
427 genes.

428           Approximately 4% (218 out of 5,423) of all the lncRNA genes in our dataset contain an exon  
429 module. Even though we cannot assign a specific function to each of these modules, as it has been  
430 done for the majority of protein coding domains, it is tempting to infer that sharing of functional modules  
431 between different lncRNAs may contribute to expanding the functional repertoire of the non-coding  
432 genome, similar to the shuffling of functional exons in coding sequences [12].

433           lncRNA exon modules identified in this work display a higher degree of sequence conservation  
434 and synteny in four primate great ape species than the remainder of lncRNA exons. A high level of  
435 conservation between related species is suggestive of purifying selection and is a landmark  
436 characteristic of functional genetic elements [52]. Exon modules also harbor a lower frequency of SNPs  
437 compared with control sequences, which suggests that purifying selection also persists intra-specifically

438 in human populations. Our set included 46 exon pairs highly similar in both sequence and structure (1F  
439 Fig.), which are associated with the highest conservation scores. Even though we cannot infer the age  
440 of the duplication/shuffling event based on our analysis, our results show that the exons involved are  
441 subjected to extreme purifying selection, which preserved both sequence and structure. Taken together,  
442 this evidence suggests that these modules play an important role within their respective lncRNA genes,  
443 even though their exact function is yet to be characterized.

444         Some of the modules may also have undergone an accelerated divergence. Our set includes  
445 219 and 75 exon pairs similar only in sequence or structure, respectively, and since our inclusion criteria  
446 considered both similarity and evolutionary conservation, examples of accelerated evolution may have  
447 escaped our search. This mechanism is equally relevant, especially when searching for evolutionary  
448 innovations specific to the human lineage. However, different methods than those used here are  
449 required to identify such cases. Finally, it was reported that homologous lncRNAs can, in some cases,  
450 conserve their function over long evolutionary times, despite having diverged in both their nucleotide  
451 sequences and their secondary structures [53]. The above considerations suggest that our analysis may  
452 underestimate the extent of module sharing in lncRNAs. Other limitations include the fact that the correct  
453 identification of exons within lncRNAs is strongly dependent on the reliability of the reconstruction of the  
454 whole transcript structure. This is usually summarized by the TSL parameter (Transcript Support Level)  
455 which we included, for every exon, in the Supporting information (S1 Table).

456         In the few cases for which functional information on a lncRNA is available, it may be possible to  
457 infer the function of the shared module. We report two examples of modules conserved in either  
458 sequence or structure. In both cases, the ability to bind specific targets is the inferred associated  
459 function.

460         Overall, our results highlight the presence of groups of exons sharing high sequence or structure  
461 similarity within dissimilar lncRNA genes. These exons are highly conserved across primate species  
462 and depleted of inter-individual variation among humans (SNPs), and we suggest that they may  
463 represent functional modules.

464         The identification of these modules could constitute a tool for decoding the function of the many  
465 lncRNAs that are currently uncharacterized. Membership in a shared exon cluster represents a feature  
466 that deserves annotation, even though conclusive proof of shared function will require experimental  
467 evidence.

468

## 469 **Materials and Methods**

470

### 471 **Dataset**

472

473 We used gencode version 29 [3], to select 34,509 exons annotated as long intergenic non-  
474 coding RNA, which do not have overlaps with protein coding genes, and downloaded their chromosomal  
475 coordinates as a gtf file. We then used these coordinates to obtain the corresponding sequences from  
476 the hg38 version of the human genome (UCSC genome browser), converting the gtf to bed file and  
477 using the getfasta tool from the bedtools suite [54], with repetitive sequences masked by RepeatMasker  
478 (Smit et al., unpublished data, [www.repeatmasker.org](http://www.repeatmasker.org)) and Tandem Repeats Finder [55]. We removed  
479 18,703 exons containing repetitive sequences and retained 15,806 exons. 3,709 of these were shared  
480 by different isoforms of the same lncRNA gene. In such cases we only considered the longest isoform,  
481 thus obtaining a final set of 12,097 non-overlapping exons that do not contain repetitive sequences.  
482 These exons belong to 5,423 different lncRNA genes.

483

### 484 **Sequence alignments**

485

486 All exon sequences were compared to each other using the Needleman and Wunsch global  
487 alignment algorithm [56], using the same default gap penalties scores as the EMBOSS Needle tool for  
488 global alignments of nucleic acids sequences [57] (-10 for gap insertions, -0.5 for gap extensions) and  
489 the EDNAFULL substitution matrix.

490

### 491 **Structure alignments**

492

493 The secondary structure of each exon was calculated using RNAfold [57,58], as the minimum  
494 free energy (MFE) structure, and represented by its dot-bracket notation. These representations were  
495 converted into the BEAR alphabet for RNA secondary structure notation (Mattei et al. 2014). The BEAR

496 alphabet is an encoding method for RNA secondary structure, whose characters encode for a specific  
497 secondary structure element (loop, stem, bulge and internal loop) with specific length (e.g. a nucleotide  
498 that is part of a stem of length 5 is represented by one character and a different character is used to  
499 represent a stem of a different length). The global structure alignments were performed using the  
500 BEAGLE algorithm [59], with default parameters (-2 for gap insertions, -0.7 for gap extensions, +0.6 for  
501 the sequence match bonus) and the substitution matrix for RNA structural elements (MBR, Matrix of  
502 Bear-encoded RNAs) described in [50]. To avoid favoring alignments between unstructured regions we  
503 modified the original MBR, assigning a score of 0 to matches in these regions. BEAGLE is an algorithm  
504 for pairwise RNA secondary structure global comparison similar to the Needleman and Wunsch  
505 algorithm for sequence alignments.

506 For both sequence and structure alignments we considered the scores of the aligned sequences  
507 after trimming external gaps. The score of each alignment was normalized by its length, to avoid biases  
508 towards longer sequences. We selected only alignments of a length of at least 50 nucleotides after the  
509 external gap trimming. The final distributions consisted of approx. 73 million values, with z-scores  
510 ranging from  $\sim -36$  to  $\sim -16$  and from  $\sim -3$  to  $\sim 9$ , respectively.

511

## 512 **Repetitive elements and cis-regulatory elements**

513

514 Repetitive sequences were mapped using the rmsk table from the UCSC genome browser,  
515 which is derived from RepeatMasker (Smit et al., unpublished data, [www.repeatmasker.org](http://www.repeatmasker.org)).

516 Cis-regulatory elements coordinates are derived from the ENCODE Registry of candidate cis-  
517 Regulatory Elements (cCREs) combined from all human cell types [60]. The enrichments are calculated  
518 using a Fisher's exact test between modules containing a particular CRE and the other lncRNA exons  
519 of the dataset with a Benjamini-Hochberg correction.

520

## 521 **Evolutionary conservation score**

522

523 The evolutionary conservation score for each exon was calculated using an approach similar to  
524 [61], using the BLAST+ suite of command-line tools [62]. More specifically, the BLASTn algorithm was



525 used to perform an alignment of all the lncRNA exons of our dataset (12,097). In view of the pattern of  
526 the evolutionary conservation of lncRNA sequences [14], we used the genomes of four primate species  
527 closely related to *H. sapiens*: *Pan troglodytes* (Chimpanzee, taxid:9598), *Pan paniscus* (Bonobo,  
528 taxid:9597), *Pongo pygmaeus* (Orangutan, taxid:9601) and *Gorilla gorilla* (Gorilla, taxid:9592). For each  
529 lncRNA exon we then calculated a comprehensive conservation score as the sum of the best match bit-  
530 score over the four species, divided by the length of the query sequence. Though the four organisms  
531 are phyletically correlated, we used this procedure to buffer lineage-specific effects and potential  
532 genome annotation errors.

533 For both sequence and structure similarity scores, the resulting distributions were compared  
534 with the inter-specific degree of sequence conservation, under the hypothesis that constraints on exon  
535 variation acted both intra- and inter-specifically. These comparisons were used to explore the  
536 relationship between intra- and inter-specific conservation scores around the z-score value of 6.0  
537 proposed by [63] as the threshold to distinguish homologous sequences (1 Fig.).

538 We excluded from this comparison exon pairs located in genes that are globally similar as the  
539 similarity of the exons would simply reflect gene paralogy. To do so we performed a pairwise alignment  
540 of the genes containing the exon pairs using BLASTn. The genomic coordinates of the whole genes,  
541 including the introns, were retrieved from the gencode version 29 gtf file [3], and we used the same  
542 procedure described above for the exons to obtain their sequences. Local alignments were performed  
543 considering the smallest gene of the pair as the query and the longest as the subject, and excluding  
544 pairs presenting a total query coverage greater than or equal to 80%. For each exon pair, we also  
545 checked the coordinates from the bed file, excluding overlapping pairs.

546

## 547 **Syntenies**

548

549 Synteny data were collected from SyntDB [32], which takes into account positional conservation  
550 and sequence similarity to identify syntenic regions of human lncRNAs across primates. This database  
551 comprises synteny information for 55632 transcripts. From this dataset we selected conservation data  
552 in Chimpanzee, Bonobo, Orangutan and Gorilla for the 8,390 lncRNA transcripts containing the 12,097  
553 exons in our dataset.

554

## 555 **Single nucleotide polymorphisms (SNPs)**

556

557           SNPs locations were retrieved from common dbSNP 153 (variants with a minor allele frequency  
558 (MAF) of at least 1% (0.01) in the 1000 Genomes Phase 3 dataset) [35] and population frequencies  
559 were obtained from the ALFA allele frequency aggregator project [36]. The release 2 vcf format file  
560 contains variant frequency data aggregated from 79 different studies on more than 900 million SNPs.  
561 We used the tabix tool from the SAMtools suite of programs [64] to select SNPs located within one of  
562 the 12,097 exons in our dataset, obtaining ~764,000 variants with associated allele frequency  
563 information.

564

## 565 **Transition/transversion ratio**

566

567           The transitions to transversion ratio (Ti/Tv) was calculated by using the variant data present in  
568 the common dbSNP 153 (see above) for all the 12,097 lncRNA exons in our dataset, as the number of  
569 pyrimidine-pyrimidine or purine-purine substitutions (transitions), divided by the number of purine-  
570 pyrimidine or pyrimidine-purine substitutions (transversions).

571

## 572 **Protein coding exons**

573

574           The protein coding exon coordinates were obtained from the gencode version 29 annotation  
575 and mapped on the hg38 version of the human genome using the same procedure described for the  
576 lncRNA exons.

577

## 578 **Motifs scan**

579

580           The search for sequence and structure motifs in the putative LIN28B binding module was  
581 performed using the BRIO (BEAM RNA Interaction mOtifs) web server [65]. This tool enables the  
582 identification of RNA sequence and structure motifs involved in protein binding in one or more input RNA

583 molecules, by measuring, through a Fisher's exact test, their enrichment compared to a background of  
584 RNAs from Rfam with similar length and structure content, defined as the fraction of paired nucleotides  
585 in the RNA secondary structure. The database of motifs that is included in BRIO is derived from high  
586 throughput protein-RNA binding experiments (PAR-CLIP, eCLIP and HITS) analyzed in [44]. For this  
587 analysis, we considered the default enrichment significance threshold of  $p\text{-value} < 0.05$  to evaluate the  
588 enrichment of a motif in a group of exon modules. We chose to use this algorithm because in addition  
589 to identifying common motifs on some particular modules, it allows us to associate them with motifs  
590 enriched in RNA that interact with specific proteins from experimental data.

591

## 592 **Funding**

593

594           Funded by the European Union – NextGenerationEU: National Center for Gene Therapy and  
595 Drugs based on RNA Technology, CN3 – Spoke 7 (code:CN0000041) to MHC and PFG and AIRC  
596 grant number IG 23539 project to MHC.

597

## 598 **Author Contributions**

599

600 Conceptualization: Francesco Ballesio, Gerardo Pepe, Gabriele Ausiello, Andrea Novelletto, Manuela  
601 Helmer-Citterich, Pier Federico Gherardini.

602 Data curation: Francesco Ballesio.

603 Investigation: Francesco Ballesio.

604 Funding acquisition: Manuela Helmer-Citterich, Pier Federico Gherardini.

605 Writing – original draft: Francesco Ballesio.

606 Writing – review & editing: Gerardo Pepe, Gabriele Ausiello, Manuela Helmer-Citterich, Pier Federico  
607 Gherardini, Andrea Novelletto.

608

609 Gabriele Ausiello, Manuela Helmer-Citterich, Pier Federico Gherardini, Andrea Novelletto are senior  
610 authors.

611

## 612 **Data Availability**

613

614 The annotation was obtained from GENCODE v29

615 ([https://www.gencodegenes.org/human/release\\_29.html](https://www.gencodegenes.org/human/release_29.html)).

616 The hg38 version of the human genome was downloaded from UCSC genome browser

617 (<http://hgdownload.cse.ucsc.edu/goldenPath/hg38/bigZips/>).

618 The BEAGLE webserver for RNA structure alignments is available at:

619 <http://beagle.bio.uniroma2.it>.

620 Functionally annotated lncRNA was downloaded from: <http://bio->

621 [bigdata.hrbmu.edu.cn/lnc2cancer](http://bigdata.hrbmu.edu.cn/lnc2cancer).

622 Variant frequencies in human populations are available in the ncbi website

623 (<https://www.ncbi.nlm.nih.gov/snp/docs/gsr/alfa/#ftp-download>).

624 The BRIO webserver for RNA interaction motif search is available at:

625 <http://brio.bio.uniroma2.it>.

626 SynthDB is available at: <http://syntdb.amu.edu.pl>.

627 For a list of the 340 exon pairs identified see S1 Table.

628

## 629 **Supporting information**

630

631 S1 Fig. Numerosity of lncRNA exons per exon cluster.

632 S2 Fig. Positions of the exon modules on the human chromosomes

633 S3 Fig. Comparison of BLAST hit frequencies at different evolutionary divergence ages of

634 exonic modules (A) and lncRNAs genes analyzed by Sarropoulos et al. (B).

635 S1 Table A list of identified exonic modules and their properties.

636 S2 Table Repetitive elements in the regions flanking the exonic modules.

637 S3 Table Percentage of transposase domains identified in genes containing exon modules  
638 and in other lncRNA genes.

639

## 640 **References**

641 1. Gilbert W. Why genes in pieces? In: Nature Publishing Group UK [Internet]. 1 Feb 1978  
642 [cited 23 Oct 2023]. doi:10.1038/271501a0

643 2. Engreitz JM, Haines JE, Perez EM, Munson G, Chen J, Kane M, et al. Local regulation  
644 of gene expression by lncRNA promoters, transcription and splicing. *Nature*. 2016;539:  
645 452–455.

646 3. Frankish A, Diekhans M, Jungreis I, Lagarde J, Loveland JE, Mudge JM, et al.  
647 GENCODE 2021. *Nucleic Acids Res*. 2021;49: D916–D923.

648 4. Quek XC, Thomson DW, Maag JLV, Bartonicek N, Signal B, Clark MB, et al. lncRNADB  
649 v2.0: expanding the reference database for functional long noncoding RNAs. *Nucleic  
650 Acids Res*. 2015;43: D168–73.

651 5. Gao Y, Shang S, Guo S, Li X, Zhou H, Liu H, et al. lnc2Cancer 3.0: an updated  
652 resource for experimentally supported lncRNA/circRNA cancer associations and web  
653 tools based on RNA-seq and scRNA-seq data. *Nucleic Acids Res*. 2021;49: D1251–  
654 D1258.

655 6. Fort V, Khelifi G, Hussein SMI. Long non-coding RNAs and transposable elements: A  
656 functional relationship. *Biochim Biophys Acta Mol Cell Res*. 2021;1868: 118837.

657 7. Ponting CP, Oliver PL, Reik W. Evolution and functions of long noncoding RNAs. *Cell*.  
658 2009;136: 629–641.

659 8. Statello L, Guo C-J, Chen L-L, Huarte M. Gene regulation by long non-coding RNAs and

- 660 its biological functions. *Nat Rev Mol Cell Biol.* 2021;22: 96–118.
- 661 9. Gupta RA, Shah N, Wang KC, Kim J, Horlings HM, Wong DJ, et al. Long non-coding  
662 RNA HOTAIR reprograms chromatin state to promote cancer metastasis. *Nature.*  
663 2010;464: 1071–1076.
- 664 10. Ng S-Y, Johnson R, Stanton LW. Human long non-coding RNAs promote pluripotency  
665 and neuronal differentiation by association with chromatin modifiers and transcription  
666 factors. *EMBO J.* 2012;31: 522–533.
- 667 11. Faghihi MA, Modarresi F, Khalil AM, Wood DE, Sahagan BG, Morgan TE, et al.  
668 Expression of a noncoding RNA is elevated in Alzheimer’s disease and drives rapid  
669 feed-forward regulation of beta-secretase. *Nat Med.* 2008;14: 723–730.
- 670 12. Guttman M, Rinn JL. Modular regulatory principles of large non-coding RNAs. *Nature.*  
671 2012;482: 339–346.
- 672 13. Ulitsky I, Bartel DP. lincRNAs: genomics, evolution, and mechanisms. *Cell.* 2013;154:  
673 26–46.
- 674 14. Johnsson P, Lipovich L, Grandér D, Morris KV. Evolutionary conservation of long non-  
675 coding RNAs; sequence, structure, function. *Biochim Biophys Acta.* 2014;1840: 1063–  
676 1071.
- 677 15. Ulitsky I, Shkumatava A, Jan CH, Sive H, Bartel DP. Conserved function of lincRNAs in  
678 vertebrate embryonic development despite rapid sequence evolution. *Cell.* 2011;147:  
679 1537–1550.
- 680 16. Kelley D, Rinn J. Transposable elements reveal a stem cell-specific class of long  
681 noncoding RNAs. *Genome Biol.* 2012;13: R107.
- 682 17. Fueyo R, Judd J, Feschotte C, Wysocka J. Roles of transposable elements in the  
683 regulation of mammalian transcription. *Nat Rev Mol Cell Biol.* 2022;23: 481–497.

- 684 18. Johnson R, Guigó R. The RIDL hypothesis: transposable elements as functional  
685 domains of long noncoding RNAs. *RNA*. 2014;20: 959–976.
- 686 19. Kapusta A, Kronenberg Z, Lynch VJ, Zhuo X, Ramsay L, Bourque G, et al. Transposable  
687 elements are major contributors to the origin, diversification, and regulation of vertebrate  
688 long noncoding RNAs. *PLoS Genet*. 2013;9: e1003470.
- 689 20. Kirk JM, Kim SO, Inoue K, Smola MJ, Lee DM, Schertzer MD, et al. Functional  
690 classification of long non-coding RNAs by k-mer content. *Nat Genet*. 2018;50: 1474–  
691 1482.
- 692 21. Martin L, Meier M, Lyons SM, Sit RV, Marzluff WF, Quake SR, et al. Systematic  
693 reconstruction of RNA functional motifs with high-throughput microfluidics. *Nat Methods*.  
694 2012;9: 1192–1194.
- 695 22. Muckenthaler MU, Galy B, Hentze MW. Systemic iron homeostasis and the iron-  
696 responsive element/iron-regulatory protein (IRE/IRP) regulatory network. *Annu Rev Nutr*.  
697 2008;28: 197–213.
- 698 23. Zhang C, Lee K-Y, Swanson MS, Darnell RB. Prediction of clustered RNA-binding  
699 protein motif sites in the mammalian genome. *Nucleic Acids Res*. 2013;41: 6793–6807.
- 700 24. Oberstrass FC, Lee A, Stefl R, Janis M, Chanfreau G, Allain FH-T. Shape-specific  
701 recognition in the structure of the Vts1p SAM domain with RNA. *Nat Struct Mol Biol*.  
702 2006;13: 160–167.
- 703 25. Gustavsen JA, Pai S, Isserlin R, Demchak B, Pico AR. RCy3: Network biology using  
704 Cytoscape from within R. *F1000Res*. 2019;8: 1774.
- 705 26. Bailey JA, Gu Z, Clark RA, Reinert K, Samonte RV, Schwartz S, et al. Recent segmental  
706 duplications in the human genome. *Science*. 2002;297: 1003–1007.
- 707 27. Antonarakis SE. Content and variation of the human genome. *Medical and Health*

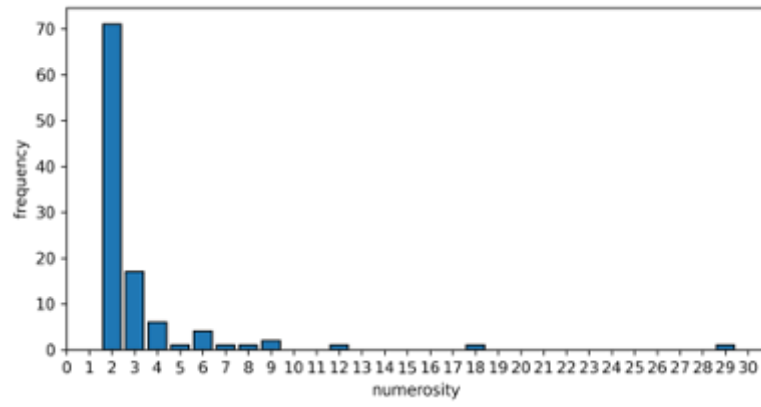
- 708 Genomics. Elsevier; 2016. pp. 161–177.
- 709 28. Abdullaev ET, Umarova IR, Arndt PF. Modelling segmental duplications in the human  
710 genome. *BMC Genomics*. 2021;22: 496.
- 711 29. Koch L. Capturing transposases for new proteins. *Nature reviews. Genetics*. 2021. pp.  
712 266–267.
- 713 30. Li B, Carey M, Workman JL. The role of chromatin during transcription. *Cell*. 2007;128:  
714 707–719.
- 715 31. Toll-Riera M, Albà MM. Emergence of novel domains in proteins. *BMC Evol Biol*.  
716 2013;13: 1–10.
- 717 32. Bryzghalov O, Szcześniak MW, Makałowska I. SyntDB: defining orthologues of human  
718 long noncoding RNAs across primates. *Nucleic Acids Res*. 2020;48: D238–D245.
- 719 33. Sarropoulos I, Marin R, Cardoso-Moreira M, Kaessmann H. Developmental dynamics of  
720 lncRNAs across mammalian organs and species. *Nature*. 2019;571: 510–514.
- 721 34. Cvijović I, Good BH, Desai MM. The Effect of Strong Purifying Selection on Genetic  
722 Diversity. *Genetics*. 2018;209: 1235–1278.
- 723 35. Sherry ST, Ward M-H, Kholodov M, Baker J, Phan L, Smigielski EM, et al. dbSNP: the  
724 NCBI database of genetic variation. *Nucleic Acids Res*. 2001;29: 308–311.
- 725 36. Phan, Jin, Zhang, Qiang, Shekhtman, Shao, et al. ALFA: allele frequency aggregator.  
726 National Center for Biotechnology Information, US National Library of Medicine.
- 727 37. Nei M. *Molecular Evolutionary Genetics*. New York Chichester, West Sussex: Columbia  
728 University Press; 1987.
- 729 38. França GS, Cancherini DV, de Souza SJ. Evolutionary history of exon shuffling.  
730 *Genetica*. 2012;140: 249–257.



- 731 39. Yang Z, Bielawski JP. Statistical methods for detecting molecular adaptation. Trends  
732 Ecol Evol. 2000;15: 496–503.
- 733 40. Wang J, Raskin L, Samuels DC, Shyr Y, Guo Y. Genome measures used for quality  
734 control are dependent on gene function and ancestry. Bioinformatics. 2015;31: 318–323.
- 735 41. Takei Y, Ishikawa S, Tokino T, Muto T, Nakamura Y. Isolation of a novel TP53 target  
736 gene from a colon cancer cell line carrying a highly regulated wild-type TP53 expression  
737 system. Genes Chromosomes Cancer. 1998;23: 1–9.
- 738 42. Diaz-Lagares A, Crujeiras AB, Lopez-Serra P, Soler M, Setien F, Goyal A, et al.  
739 Epigenetic inactivation of the p53-induced long noncoding RNA TP53 target 1 in human  
740 cancer. Proc Natl Acad Sci U S A. 2016;113: E7535–E7544.
- 741 43. Finkbeiner MR, Astanehe A, To K, Fotovati A, Davies AH, Zhao Y, et al. Profiling YB-1  
742 target genes uncovers a new mechanism for MET receptor regulation in normal and  
743 malignant human mammary cells. Oncogene. 2009;28: 1421–1431.
- 744 44. Adinolfi M, Pietrosanto M, Parca L, Ausiello G, Ferrè F, Helmer-Citterich M. Discovering  
745 sequence and structure landscapes in RNA interaction motifs. Nucleic Acids Res.  
746 2019;47: 4958–4969.
- 747 45. Lin X, Shen J, Dan Peng, He X, Xu C, Chen X, et al. RNA-binding protein LIN28B  
748 inhibits apoptosis through regulation of the AKT2/FOXO3A/BIM axis in ovarian cancer  
749 cells. Signal Transduct Target Ther. 2018;3: 23.
- 750 46. Wilbert ML, Huelga SC, Kapeli K, Stark TJ, Liang TY, Chen SX, et al. LIN28 binds  
751 messenger RNAs at GGAGA motifs and regulates splicing factor abundance. Mol Cell.  
752 2012;48: 195–206.
- 753 47. Piskounova E, Polytarchou C, Thornton JE, LaPierre RJ, Pothoulakis C, Hagan JP, et al.  
754 Lin28A and Lin28B inhibit let-7 microRNA biogenesis by distinct mechanisms. Cell.

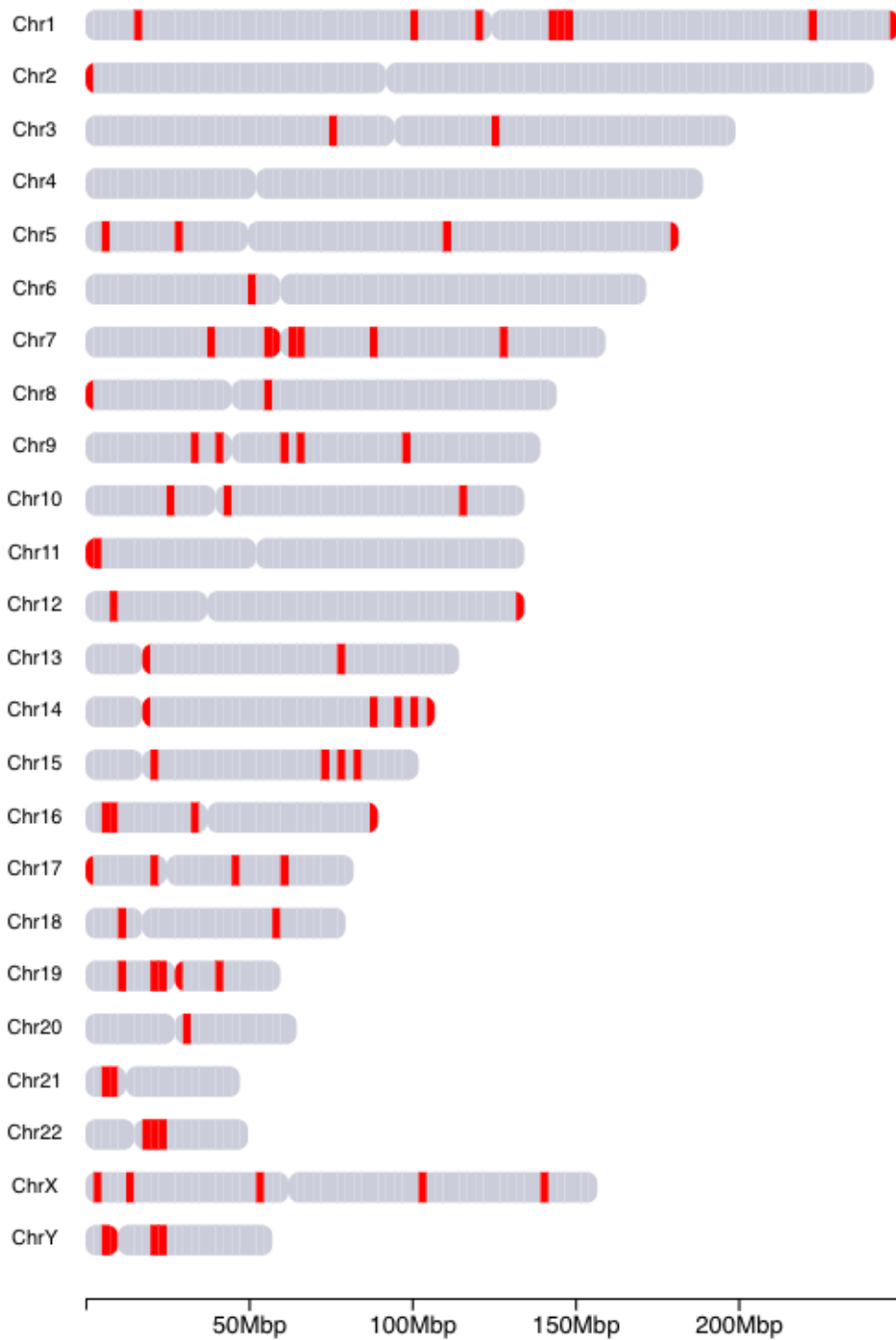
- 755           2011;147: 1066–1079.
- 756   48. Yong W, Yu D, Jun Z, Yachen D, Weiwei W, Midie X, et al. Long noncoding RNA  
757       NEAT1, regulated by LIN28B, promotes cell proliferation and migration through sponging  
758       miR-506 in high-grade serous ovarian cancer. *Cell Death Dis.* 2018;9: 861.
- 759   49. Peters DT, Fung HKH, Levdivkov VM, Imscher T, Warrander FC, Greive SJ, et al.  
760       Human Lin28 Forms a High-Affinity 1:1 Complex with the 106~363 Cluster miRNA miR-  
761       363. *Biochemistry.* 2016;55: 5021–5027.
- 762   50. Mattei E, Ausiello G, Ferrè F, Helmer-Citterich M. A novel approach to represent and  
763       compare RNA secondary structures. *Nucleic Acids Res.* 2014;42: 6146–6157.
- 764   51. Crooks GE, Hon G, Chandonia J-M, Brenner SE. WebLogo: a sequence logo generator.  
765       *Genome Res.* 2004;14: 1188–1190.
- 766   52. Kellis M, Wold B, Snyder MP, Bernstein BE, Kundaje A, Marinov GK, et al. Defining  
767       functional DNA elements in the human genome. *Proc Natl Acad Sci U S A.* 2014;111:  
768       6131–6138.
- 769   53. Karner H, Webb C-H, Carmona S, Liu Y, Lin B, Erhard M, et al. Functional Conservation  
770       of LncRNA JPX Despite Sequence and Structural Divergence. *J Mol Biol.* 2020;432:  
771       283–300.
- 772   54. Quinlan AR, Hall IM. BEDTools: a flexible suite of utilities for comparing genomic  
773       features. *Bioinformatics.* 2010;26: 841–842.
- 774   55. Benson G. Tandem repeats finder: a program to analyze DNA sequences. *Nucleic Acids*  
775       *Res.* 1999;27: 573–580.
- 776   56. Needleman SB, Wunsch CD. A general method applicable to the search for similarities  
777       in the amino acid sequence of two proteins. *J Mol Biol.* 1970;48: 443–453.

- 778 57. Rice P, Longden I, Bleasby A. EMBOSS: the European Molecular Biology Open  
779 Software Suite. *Trends Genet.* 2000;16: 276–277.
- 780 58. Lorenz R, Bernhart SH, Höner Zu Siederdisen C, Tafer H, Flamm C, Stadler PF, et al.  
781 ViennaRNA Package 2.0. *Algorithms Mol Biol.* 2011;6: 26.
- 782 59. Mattei E, Pietrosanto M, Ferrè F, Helmer-Citterich M. Web-Beagle: a web server for the  
783 alignment of RNA secondary structures. *Nucleic Acids Res.* 2015;43: W493–7.
- 784 60. Moore JE, Purcaro MJ, Pratt HE, Epstein CB, Shores N, Adrian J, et al. Expanded  
785 encyclopaedias of DNA elements in the human and mouse genomes. *Nature.* 2020;583:  
786 699–710.
- 787 61. Jha A, Quesnel-Vallières M, Wang D, Thomas-Tikhonenko A, Lynch KW, Barash Y.  
788 Identifying common transcriptome signatures of cancer by interpreting deep learning  
789 models. *Genome Biol.* 2022;23: 117.
- 790 62. Camacho C, Coulouris G, Avagyan V, Ma N, Papadopoulos J, Bealer K, et al. BLAST+:  
791 architecture and applications. *BMC Bioinformatics.* 2009;10: 421.
- 792 63. Mitrophanov AY, Borodovsky M. Statistical significance in biological sequence analysis.  
793 *Brief Bioinform.* 2006;7: 2–24.
- 794 64. Danecek P, Bonfield JK, Liddle J, Marshall J, Ohan V, Pollard MO, et al. Twelve years of  
795 SAMtools and BCFtools. *Gigascience.* 2021;10. doi:10.1093/gigascience/giab008
- 796 65. Guarracino A, Pepe G, Ballesio F, Adinolfi M, Pietrosanto M, Sangiovanni E, et al. BRIO:  
797 a web server for RNA sequence and structure motif scan. *Nucleic Acids Res.* 2021;49:  
798 W67–W71.
- 799
- 800



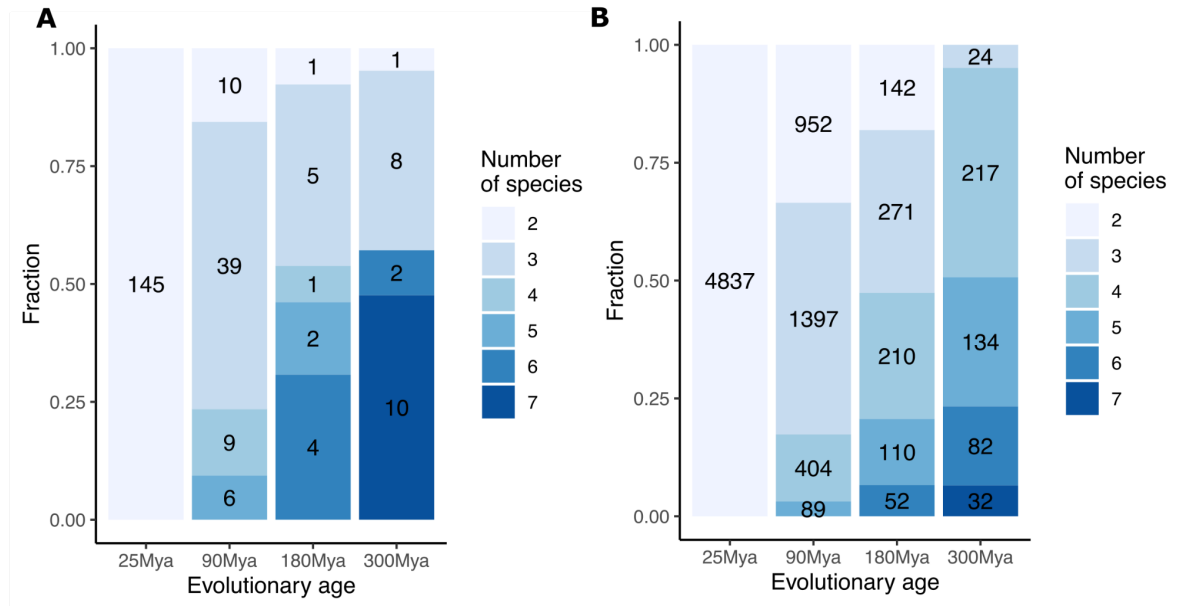
801

802 Fig. S1 - Numerosity of IncRNA exons per exon cluster.



803

804 Fig. S2 - Positions of the exon modules on the human chromosomes



805

806 Fig. S3 - Comparison of BLAST hit frequencies at different evolutionary divergence ages of  
807 exonic modules (A) and lncRNAs genes analyzed by Sarropoulos et al. (B).